DOI: 10.1002/ejic.200600519

Transition-Metal (Mn^{II} and Co^{II}) Complexes with the Heteropolymolybdate Fragment $[As^{V}Mo_9O_{33}]^{7-}$: Crystal Structures, Electrochemical and Magnetic Properties

Yanyan Yang,[a] Lin Xu,*[a] Guanggang Gao,[a] Fengyan Li,[a] Yunfeng Qiu,[a] Xiaoshu Qu,[a] and Hong Liu[a]

Keywords: Polyoxometalates / Molybdenum / Arsenic / Magnetic properties

Two novel heteropolymolybdates, $[(CH_3)_4N]_{8n}[M(H_2O)_5]_{2n}(H_3O)_{2n}[\{M(H_2O)_5\}_2(MAs^{V}Mo_9O_{33})_2]_n[M(H_2O)_4(MAs^{V}Mo_9O_{33})_2]_n{\cdot}20nH_2O$ (M = Mn^{2+}, **1**; M = Co^{2+}, **2**), constructed from the new fragment $(As^{V}Mo_9O_{33})^{7-}$ and a transition metal have been synthesized in aqueous solution and characterized by elemental analysis, IR spectroscopy, thermal gravimetric analysis, and single-crystal X-ray diffraction. Structurally the title complexes resemble a sandwich-type complex because they involve the coordination of two transition metals to two $[As^{V}Mo_9O_{33}]^{7-}$ fragments, which derive from the well-known *B*-β-Keggin structure. Compounds **1** and **2** exhibit a one-dimensional chain-like framework $[M(H_2O)_4(MAs^{V}Mo_9O_{33})_2]^{8n-}$ with isolated $\{[M(H_2O)_5]_2(MAs^{V}Mo_9O_{33})_2\}^{6-}$ units residing among the chains. The magnetic properties of the two complexes were investigated to indicate typical antiferromagnetic interactions through the Mn^{II}–O–Mn^{II} bridge unit for complex **1** and the Co^{II}–O–Co^{II} bridge unit for complex **2**.

Introduction

Polyoxometalates (POMs), a well-known class of metal oxygen clusters with a large variety of compositions and structures, together with their physicochemical properties, are of considerable interest because of their potential application in areas of catalysis, materials science, medicine, and so forth.[1–7] In virtue of a great family of POM building blocks, significant effort has gone into creating rational assemblies to obtain new compounds with desired functional properties. In the class of polyoxometalates, the sandwich-type complexes consisting of polyoxometalates and a transition-metal ion are an important subfamily because of their structural and magnetic diversity.[8–12] Recently, the sandwich-type complexes based on the lacunary heteropolytungstates have been synthesized and structurally characterized in increasing numbers.[13–15] In addition, among the sandwich-type complexes, a large number of magnetic clusters with various nuclearities and original topologies were formed by using the lacunary heteropolytungstates as the main ligand units. In contrast with the above situation, a true heteropolymolybdate analogue of a sandwich-type cluster has not been reported so far, and only a heteropolymolybdate formulated as $[Cu_2(SiMo_9O_{33})_2]^{12-}$, whose structure resembles a sandwich-type POM cluster, has been isolated and structurally characterized since 1981.[16] Why has only one example of a heteropolymolybdate with this structure appeared in the past 25 years? This is mainly because the lacunary heteropolymolybdate behaves with structural lability in aqueous solution, so that the isolation of a stable sandwich-type complex of lacunary heteropolymolybdate is considerably difficult. Müller and co-workers reported the existence of an $\{As^{III}Mo_9O_{33}\}$ fragment in the complexes $K_7[(AsOH)_3(MoO_3)_3(AsMo_9O_{33})]{\cdot}15H_2O$, $K_{10}[(AsOH)_6(MoO_3)_2(O_2Mo{-}O{-}MoO_2)_2(AsMo_9O_{33})_2]{\cdot}12H_2O$, and $(HNMe_3)_8[H_6As_{10}Mo_{24}O_{90}]{\cdot}9H_2O$,[17,18] but the $\{As^{III}Mo_9O_{33}\}$ fragment can rapidly rearrange into a Keggin-type cluster of $\{As^{V}Mo_{12}O_{40}\}$, suggesting that it is very difficult to obtain complexes consisting of the $\{As^{V}Mo_9O_{33}\}$ fragment from aqueous solution. Hence, the successful synthesis of a heteropolymolybdate-based sandwich complex remains a challenge. In particular, the complexes consisting of both heteropolymolybdates and a transition metal may produce unexpected magnetic properties, providing a great opportunity to explore heteropolymolybdate-based magnetic materials.

In our work, we try to find the rational reaction condition to obtain stable sandwich-type complexes consisting of heteropolymolybdates and a transition metal. Herein we report the syntheses, crystal structures, and magnetic properties of two new complexes consisting of arsenomolybdates and transition metals, $[(CH_3)_4N]_{8n}[M(H_2O)_5]_{2n}(H_3O)_{2n}$-

[a] Key Laboratory of Polyoxometalates Science of Ministry of Education,
College of Chemistry, Northeast Normal University,
Changchun 130024, P.R. China
E-mail: linxu@nenu.edu.cn

Supporting information for this article is available on the WWW under http://www.eurjic.org or from the author.

$[\{M(H_2O)_5\}_2(MAs^{V}Mo_9O_{33})_2]_n[M(H_2O)_4(MAs^{V}Mo_9O_{33})_2]_n\cdot 20nH_2O$, in which two crystallographically independent $[\{M(H_2O)_5\}_2(MAs^{V}Mo_9O_{33})_2]^{6-}$ (**1a**) and $[M(H_2O)_4(MAs^{V}Mo_9O_{33})_2]^{8n-}$ (**1b**) units coexist in their crystal structure. Notably, the complexes structurally resemble a sandwich-type complex because they involve the coordination of two transition metals to two $[As^{V}Mo_9O_{33}]^{7-}$ fragments, and the $[As^{V}Mo_9O_{33}]^{7-}$ fragment in **1** and **2** is not an ordinary trivacant α-Keggin ion but a special derivative of the well-known *B*-β-Keggin structure. To the best of our knowledge, they represent the first example of structurally characterized complexes containing both a $\{As^{V}Mo_9O_{33}\}$ fragment and a transition metal, although the component of the unit is isostructural with the reported $[Cu_2(SiMo_9O_{33})_2]^{12-}$ anion. The physicochemical properties of the two complexes were also characterized by thermal gravimetric analysis, cyclic voltammograms, and magnetic susceptibility measurement.

Results and Discussion

In contrast to heteropolytungstates, heteropolymolybdate anions generally show more structural lability in aqueous solution, so it is very difficult to isolate a sandwich-type complex containing lacunary heteropolymolybdate species. The reaction of Mn^{2+} ions with α-$As^{V}Mo_{12}O_{40}^{3-}$ in the ratio 16:1 (pH adjusted to 4.2) produced the unexpected $[(CH_3)_4N]_{8n}[M(H_2O)_5]_{2n}(H_3O)_{2n}[\{M(H_2O)_5\}_2(MAs^{V}Mo_9O_{33})_2]_n[M(H_2O)_4(MAs^{V}Mo_9O_{33})_2]_n\cdot 20nH_2O$ (M = Mn^{2+}, **1**; M = Co^{2+}, **2**), in which the $[As^{V}Mo_9O_{33}]^{7-}$ fragment derives from the well-known (*B*-β-XMo_9O_{33}) structure, and whose structure resembles that of the sandwich-type complex. Syntheses of **1** and **2** were conveniently carried out in aqueous solution, and the key factor for the successful synthesis was a rational choice of the solution pH and a suitable countercation. A solution pH of 4.2 is appropriate for both the generation of a $[As^{V}Mo_9O_{33}]^{7-}$ fragment and the formation of complexes **1** and **2**. However, some larger countercations, such as $[Bu_4N]^+$, $[Et_4N]^+$, and Cs^+, could quickly cause the precipitation of all the cluster anions in the solution, making it impossible to obtain a stable single crystal.

Single-crystal X-ray diffraction analysis revealed that complex **1** consists of six kinds of subunits: $[\{Mn(H_2O)_5\}_2(MnAs^{V}Mo_9O_{33})_2]^{6-}$ fragment (**1a**), one-dimension chain built of $[Mn(H_2O)_4(MnAs^{V}Mo_9O_{33})_2]^{8n-}$ fragment (**1b**), $[(CH_3)_4N]^+$ cation, Mn^{2+} cation, coordinated water molecules, and isolated water molecules. The bond-valence sum calculation for complex **1** suggests that all Mo atoms are in the +6 oxidation state with an average value of 5.947, all As atoms are in the +5 oxidation state with an average value of 4.881, and all O atoms are in the –2 oxidation state with an average value of 1.964.[19] As complex **1** was isolated from acidic aqueous solution, two protons were attached to isolated water molecules to compensate for charge balance. The thermal gravimetric (TG) curve indicated the existence of 22 crystalline water molecules in complex **1**. In complex **1**, a novel building block $[\{Mn(H_2O)_5\}_2(MnAs^{V}Mo_9O_{33})_2]^{6-}$ (**1a**), whose structure is shown in Figure 1a, displays C_{2h} symmetry with a C_2 axis through two Mn^{II} centers. The building block is composed of two unusual $[As^{V}Mo_9O_{33}]^{7-}$ (**1c**) moieties linked with a $\{Mn_2O_{10}\}$ group. As shown in Scheme 1, the unusual $\{XMo_9O_{33}\}$ unit in **1c** derives from the well-known (*B*-β-XMo_9O_{33}) structure by moving one MoO_6 octahedron from the *B*-β-XMo_9O_{33} unit to the other side itself, and the MoO_6 octahedron covers what would otherwise be a hole (as compared with the Keggin structure) between the two Mo_3O_{13} units.[20] The MoO_6 octahedron has two terminal oxygen atoms, and this structural feature is similar to the first reported example of $(NH_4)_{12}[Cu_2Si_2Mo_{18}O_{66}]\cdot 14H_2O$. Also, the geometric topology of the Mn_2O_{10} group is similar to that of the $\{Cu_2O_{10}\}$ group in $(NH_4)_{12}[Cu_2Si_2Mo_{18}O_{66}]\cdot 14H_2O$. One notable feature of **1a** is that one terminal oxygen atom from the MoO_6 octahedron of two terminal oxygen atoms acts as a ligand, together with five ligand water molecules, to bond with a Mn^{2+} ion, resulting in the formation of a six-coordinate mononuclear Mn^{II} complex.

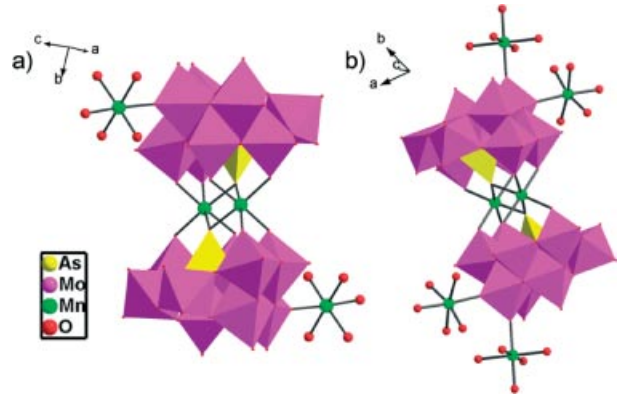

Figure 1. Combined polyhedral/ball-and-stick representation of the $[\{Mn(H_2O)_5\}_2(MnAs^{V}Mo_9O_{33})_2]^{6-}$ fragment (**1a**) and a part of the one-dimensional chain-like $[Mn(H_2O)_4(MnAs^{V}Mo_9O_{33})_2]^{8n-}$ fragment (**1b**). The color code: MoO_6 (purple), AsO_4 (yellow), Mn (green), O (red).

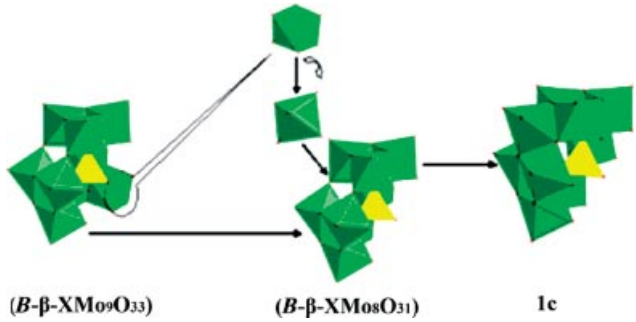

Scheme 1. The unusual $\{XMo_9O_{33}\}$ unit in **1c** derives from the well-known (*B*-β-XMo_9O_{33}) structure.

The other interesting feature of **1** is its novel one-dimensional chain structure, which consists of the **1b** unit linked by an octahedral $\{MnO_2(H_2O)_4\}$ group (see Figure 2). A

mirror plane through the chain and mononuclear Mn^{II} ions can be found if the slight deviations from two Mn–O bonds are omitted. As shown in Figure 2, the linkage between the **1b** unit and $\{MnO_2(H_2O)_4\}$ group depends entirely on a ligand oxygen atom coming from the end of a **1b** unit. It is noteworthy that the ligand oxygen atom is one of two terminal oxygen atoms from a MoO_6 octahedron of **1b**, and the other terminal oxygen atom from the MoO_6 octahedron becomes a ligand of the mononuclear Mn^{II} complex attached to the $[As^{V}Mo_9O_{33}]^{7-}$ moiety. In the mononuclear Mn^{II} complex acting as chain linker, Mn–O bond lengths related with water ligands appear to differ little [2.236(10) Å, 2.311(9) Å], while two Mn–O bond lengths related with the terminal oxygen atoms from two different MoO_6 octahedra are obviously shorter [2.130(6) Å]. It was well known that the electron delocalization generally occurs in the reduced heteropolymolybdate (heteropoly blue).[20–22] If this type of one-dimensional chain can be reduced reversibly, the additional electrons on the reduced heteropolymolybdate group will behave as electron delocalization, so that an indirect magnetic exchange interaction may happen between the magnetic groups and the reduced heteropolymolybdate groups. Thus, the development of such a magnetic chain is of considerable significance for exploring new molecular magnets. A further investigation on the heteropoly blue of **1** and its magnetic and electrochemical properties is in progress in our research group. The packing diagrams of **1** along the *a* axis are shown in Figure 2, in which those free anions of **1a** were alternately located between the parallel one-dimensional chains. In addition, all the $[(CH_3)_4N]^+$ cations, the Mn^{2+} cation and crystallized water molecules freely fill in the space of the crystal structure. Multipoint hydrogen bonds also exist between the surface oxygen atoms of the $[AsMo_9O_{33}]^{7-}$ fragment and the water molecules to stabilize the solid-state framework of **1**. The crystal structure of **2** is mostly similar to that of **1**, though the replacement of Mn^{II} by Co^{II} causes some differences in bond lengths. The two Co–O bond lengths related with the terminal oxygen atoms from two different MoO_6 octahedra are obviously shorter (2.046 Å) than the Mn–O bond lengths [2.130(6) Å]. The Co–O bond lengths related with water ligands are 2.074(13), 2.106(12), 2.074(13), and 2.106(12) Å.

The building blocks of **1a** and **1b** are composed of two $[As^{V}Mo_9O_{33}]^{7-}$ fragments derived from the well-known (*B*-β-$AsMo_9O_{33}$) structure. In polyoxoanion chemistry, this $[As^{V}Mo_9O_{33}]^{7-}$ fragment had not been observed until our work. By the same synthesis method, we have recently obtained another manganese-substituted arsenomolybdate containing the same fragment, which will be reported elsewhere. We should note that complexes **1** and **2** were synthesized from the starting material of $[\alpha\text{-}As^{V}Mo_{12}O_{40}]^{3-}$, but the resulting product was a derivative of the *B*-β-$AsMo_9O_{33}$ unit. Therefore, the mechanism of the formation of **1** and **2** must involve a loss of molybdenum atoms, rotational isomerization (α-Keggin → *B*-β-$AsMo_9O_{33}$), and metal insertion. It is not clear if **1** and **2** are formed by initial loss of molybdenum atom or first by rotational isomerization.[23]

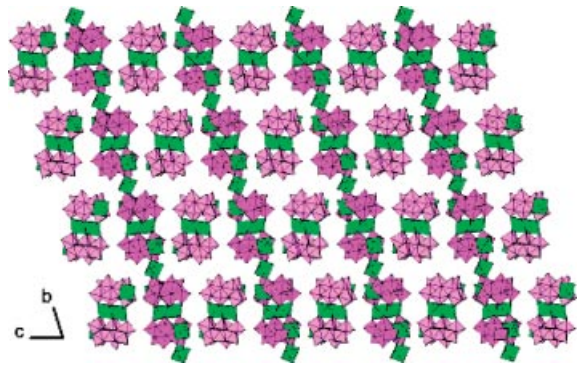

Figure 2. Polyhedral representation of plane in complexes **1** and **2**, viewed along the *a* axis. The cations and water molecules are omitted for clarity. The color code: MoO_6 (purple), MnO_6 (green).

To investigate the solution stability of complex **1**, we carried out a control measurement for the cyclic voltammograms and UV/Vis spectra in the solid state and in aqueous solutions. First, the redox peaks and shape of the cyclic voltammogram in solid state [using the carbon paste electrode (CPE)] is clearly different from those of the voltammogram in aqueous solution (1 M H_2SO_4). Second, in the UV/Vis spectra, the absorption peak positions for the solid state of complex **1** (using the diffuse reflectance electronic spectra) are also different from those for the aqueous solution of complex **1**. Thus, considering these experimental results, we infer that the one-dimensional chain-like framework of complex **1** may have been disintegrated into some fragments once it was dissolved in aqueous solution, indicating its instability in aqueous solution. However, the aqueous solution of **1** can retain stability with a pH value of 0–4; this is confirmed by the fact that the UV/Vis spectra of the solution with a pH value of 0–4 did not change when monitored for 12 h at room temperature, showing that the resulting fragments are stable in aqueous solution.

The electrochemical behavior of complex **1** was investigated using complex **1**-modified carbon paste electrode (CPE) as the working electrode to measure cyclic voltammograms both in the solid state (see Figure 3, a) and aqueous solutions (see Figure 3, b). There are only two anodic peaks in solution: E_{pa} of 284.5 and 467.9 mV. In contrast, by using the **1**-modified CPE, three reversible redox peaks appeared in the potential range from +600 to –130 mV and the peak potentials $E_{1/2} = (E_{pa} + E_{pc})/2$ are 400 (I), 262.5 (II), and –39 (III) mV (scan rate: 100 mV s^{-1}). The redox peaks I–I′ and II–II′ should be ascribed to two consecutive two-electron processes, and redox peak III–III′ should be ascribed to a one-electron process.

The thermal gravimetric (TG) curve of complex **1** exhibits two steps of weight loss in the temperature range 30–700 °C (see Figure 4, a). The first weight loss of 5.06% in the temperature range 30–191 °C corresponds to the release of 22 crystalline water molecules. The second stage, which occurs from 291 to 461 °C, is attributed to the loss of 8 organic molecules and 24 coordinated water molecules; the observed weight loss (12.89%) is in agreement with the calculated value (13.01%). The thermal gravimetric (TG) curve

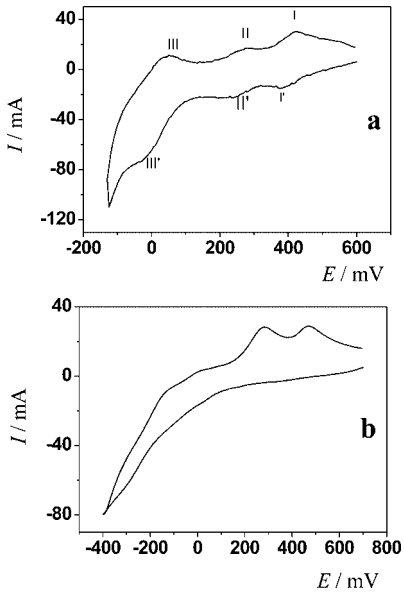

Figure 3. (a) Cyclic voltammogram of the carbon paste electrode (CPE) in 1 M H_2SO_4 aqueous solution for **1**. (b) Cyclic voltammogram of **1** in H_2SO_4 solution (pH = 2). Cyclic voltammograms were obtained with a CHI 660 electrochemical workstation at room temperature. A platinum wire was used as counter electrode and an Ag/AgCl (KCl 3 mol L^{-1}) was used as reference electrode. A chemically bulk-modified CPE or glassy carbon was used as working electrode. Potentials are quoted against a saturated calomel electrode (SCE).

of compound **2** (see Figure 4, b) is similar to that of **1**. The first weight loss of 4.97% in the temperature range 20–194 °C is attributed to the loss of crystalline water and the second weight loss of 12.79% in temperature range 300–465 °C is in agreement with the calculated value (13.84%).

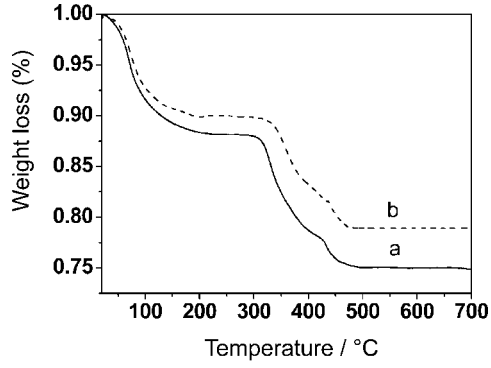

Figure 4. TGA curves of compound **1** (a) and **2** (b).

The magnetic behaviors of the two sandwich-type complexes in the temperature range 2–300 K are shown as plots of the product $\chi_m T$ versus T in Figures S12a and S12b for **1** and **2**, respectively. Because of the coexistence of dimeric and different monomeric magnetic entities in the two compounds, the exact theoretical treatment fitting the experimental data becomes practically difficult, if not impossible. The $\chi_m T$ value of complex **1** at 300 K is about 32.38 $cm^3 K mol^{-1}$ (16.09 μB); this value is slightly smaller than that expected (17.74 μB) for the isolated nine Mn^{II} ion (S = 45/2; g = 2.00). The $1/\chi_m$ versus T plot in Figure S8 for **1** displays Curie–Weiss paramagnetic behavior from 10 to 300 K. The best linear fit of $\chi_m^{-1}(T)$ data above 40 K yields C = 45.1 emu mol^{-1} and θ = –1.10 K. The experimental data can approximately be fitted to a modified Heisenberg–Dirac–Van-Vleck $\mathbf{S}_A = \mathbf{S}_B$ = 5/2 spin-coupled model assuming $\mathbf{H} = -2J\mathbf{S}_A\mathbf{S}_B$ (see Supporting Information).[24] The best fit gives magnetic coupling constant J = –0.43 cm^{-1} assuming g = 2.00, C = 82.1 emu mol^{-1}, and θ = –1.76 K, with agreement factor R {defined as $\sum_i[(\chi_m T)_{obs}(i) - (\chi_m T)_{calc}(i)]^2/\sum_i[(\chi_m T)_{obs}(i)]^2$} being 7.0×10^{-5}. The small negative J and θ values suggest the occurrence of a weak antiferromagnetic Mn^{II}–Mn^{II} interaction in **1**, being in good agreement with the result of linear fitting based on Curie–Weiss equation.

The $\chi_m T$ value of complex **2** at 300 K is about 27.59 $cm^3 K mol^{-1}$ (14.85 μB), which is higher than that expected (11.60 μB) for the isolated nine Co^{II} ion (S = 45/2; g = 2.00). The experimental magnetic data for complex **2** can approximately be fitted to a modified Heisenberg spin Hamiltonian $\mathbf{H} = -2J\mathbf{S}_A\mathbf{S}_B$ (see electronic supporting information).[25] The best fit gives magnetic coupling constant J = –0.64 cm^{-1}, g = 2.24, C = 21.61 emu mol^{-1}, and θ = –1.31 K, with agreement factor R {defined as $\sum_i[(\chi_m T)_{obs}(i) - (\chi_m T)_{calc}(i)]^2/\sum_i[(\chi_m T)_{obs}(i)]^2$} being 8.2×10^{-4} (see Figure S12). As shown in Figure S12b, the plot of $\chi_m T$ versus T for **2** shows an obvious decrease from 300 to 20 K, followed by a quick drop to 2 K, being indicative of a typical antiferromagnetic Co^{II}–Co^{II} interaction. The bridge linkage of Co^{II}–O–Co^{II} in the Co_2O_{10} group may be responsible for the behavior of antiferromagnetic interactions in **2**. In the same way, a best linear fit of $\chi_m^{-1}(T)$ data above 20 K gives C = 20.6 emu mol^{-1} and θ = –0.49 K, which is in agreement with the result from the plot of $\chi_m T$ versus T. However, a good least-squares fit for **2** cannot be achieved because of the possible deviation of the theoretical model.

Conclusions

Two unusual heteropolymolybdates, $[(CH_3)_4N]_{8n}[M(H_2O)_5]_{2n}(H_3O)_{2n}[\{M(H_2O)_5\}_2(MAs^{V}Mo_9O_{33})_2]_n[M(H_2O)_4(MAs^{V}Mo_9O_{33})_2]_n \cdot 20nH_2O$ (M = Mn^{2+}, **1**; M = Co^{2+}, **2**), were synthesized by reaction of $MnSO_4$ ($CoSO_4$) with α-$H_3As^{V}Mo_{12}O_{40} \cdot 30H_2O$ in aqueous acidic medium (pH 4.2), isolated as a mixed tetramethyl ammonium salt and characterized by single-crystal X-ray diffraction. This work shows a promising perspective to develop the class of complexes consisting of arsenomolybdates and transition metals. The two typical compounds of this class with M = Mn^{II} and Co^{II} establish a new series of heteropolymolybdate complexes based on an $[As^{V}Mo_9O_{33}]^{7-}$ fragment. The magnetic properties of the two complexes were investigated to indicate typical antiferromagnetic interaction through the Mn^{II}–O–Mn^{II} bridge unit for complex **1** and the Co^{II}–O–Co^{II} bridge unit for complex **2**.

Experimental Section

General Methods and Materials: As, Mn, Co, and Mo were determined by a Leaman inductively coupled plasma (ICP) spectrometer. IR spectra were obtained with an Alpha Centaurt FTIR spectrometer with KBr pellets in the 400–4000 cm^{-1} region. The UV/Vis spectra were recorded with a 756 CRT UV/Vis spectrophotometer with 2×10^{-6} M solutions of the relevant polyanion. Matched 1.000 cm optical path quartz cuvettes were used. The TG analyses were performed on a Perkin–Elmer TGA7 instrument in flowing N_2 with a heating rate of 10 °C min^{-1}. Cyclic voltammograms were obtained with a CHI 660 electrochemical workstation at room temperature. A platinum wire was used as counter electrode and a Ag/AgCl was used as reference electrode. A chemically bulk-modified CPE was used as working electrode. The glassy carbon samples had a diameter of 3 mm. Potentials are quoted against a saturated calomel electrode (SCE). All experiments were performed at room temperature. The polyanion precursor α-$H_3As^VMo_{12}O_{40}\cdot30H_2O$ was prepared according to the literature method.[26] The purity of α-$H_3As^VMo_{12}O_{40}\cdot30H_2O$ was checked by cyclic voltammogram. All reagents and solvents for the syntheses were purchased from commercial sources and used as received.

Synthesis of $[(CH_3)_4N]_{8n}[Mn(H_2O)_5]_{2n}(H_3O)_{2n}[\{Mn(H_2O)_5\}_2(MnAs^VMo_9O_{33})_2]_n[Mn(H_2O)_4(MnAs^VMo_9O_{33})_2]_n\cdot20nH_2O$ (1): α-$H_3As^VMo_{12}O_{40}\cdot30H_2O$ (1.78 g, 1 mmol) was dissolved in H_2O (40 mL), and $MnSO_4$ (8 mL of 1 mol L^{-1} solution) was added. The solution was heated to 60 °C on the water bath. The pH of the solution was adjusted to 4.2 by addition of the saturated $NaHCO_3$ solution, and then the color of the solution changed from yellow to orange. After 2 h, the solution was cooled to room temperature, and $(CH_3)_4NBr$ (4 mL of 1 mol L^{-1} solution) was added into the stirred solution. After about 48 h, the yellow block crystals deposited from the filtrate by evaporation at room temperature. The crystals exposed in air quickly lost luster because of the volatilization of crystallized water molecules. Elemental analysis (%): calcd. (found) for **1**: Mn 6.35 (6.40), As 3.85 (3.92), Mo 44.37 (45.20). IR (KBr disk) for **1**: $\tilde{\nu}$ = 3419, 2359, 1635, 1483, 946, 860, 787, 703, 508 cm^{-1}.

Synthesis of $[(CH_3)_4N]_{8n}[Co(H_2O)_5]_{2n}(H_3O)_{2n}[\{Co(H_2O)_5\}_2(CoAs^VMo_9O_{33})_2]_n[Co(H_2O)_4(CoAs^VMo_9O_{33})_2]_n\cdot20nH_2O$ (2): The preparation of **2** was similar to that of **1**, except that $CoSO_4$ (8 mL of 1 mol L^{-1} solution) was added. Elemental analysis (%): calcd. (found) for **2**: Co 6.78 (6.89), As 3.83 (3.89), Mo 44.17 (44.39). IR (KBr disk) for **2**: $\tilde{\nu}$ = 3419, 2360, 1616, 1483, 946, 861, 702, 508 cm^{-1}.

X-ray Crystallography: Crystal data for $[(CH_3)_4N]_{8n}[Mn(H_2O)_5]_{2n}(H_3O)_{2n}[\{Mn(H_2O)_5\}_2(MnAs^VMo_9O_{33})_2]_n[Mn(H_2O)_4(MnAs^VMo_9O_{33})_2]_n\cdot20nH_2O$ (**1**): triclinic, $P\bar{1}$ (no. 2), a = 14.2108(10) Å, b = 18.8804(13) Å, c = 22.5052(16) Å, α = 71.6940(10)°, β = 83.8250(10)°, γ = 71.5560(10)°, V = 5438.0(7) $Å^3$, ρ_{calcd} = 2.338 g cm^{-3}, 21517 independent reflections with $I > 2\sigma(I)$, $1.68 < \theta < 26.05$, 1195 parameters, final R factors R_1 = 0.0646 and wR_2 = 0.1203. Crystal data for $[(CH_3)_4N]_{8n}[Co(H_2O)_5]_{2n}(H_3O)_{2n}[\{Co(H_2O)_5\}_2(CoAs^VMo_9O_{33})_2]_n[Co(H_2O)_4(CoAs^VMo_9O_{33})_2]_n\cdot20nH_2O$ (**2**): triclinic, $P\bar{1}$ (no. 2), a = 14.102(2) Å, b = 18.880(3) Å, c = 22.783(3) Å, α = 71.074(3)°, β = 83.106(3)°, γ = 70.615(2)°, V = 5412.3(14) $Å^3$, ρ_{calcd} = 2.331 g cm^{-3}, 21504 independent reflections with $I > 2\sigma(I)$, $1.81 < \theta < 26.10$, 1168 parameters, final R factors R_1 = 0.0664 and wR_2 = 0.1311. The X-ray crystallographic data were collected at 183 K for **1** and **2** on a Bruker SMART CCD single-crystal diffractometer using Mo-K_α radiation (0.71073 Å). Direct methods were used to solve the structure and to locate the heavy atoms (SHELX97). Both compounds exhibit some disorder in the range of counterions and water molecules, as is often the case with polyoxometalates. Some of the oxygen atoms are disordered, which indicates that the quality of **1** is rather poor. Although we have repeated the experiment a few times, the suitable single crystal data cannot be obtained yet. This is most likely due to the result of the low-quality single crystals (thin plates). Nevertheless, the identity of fragment **2** was clearly established (Table 1).

Table 1. Crystal data and structure refinement for compounds **1** and **2**.

	1	**2**
Empirial formula	$C_{32}H_{190}As_4Mn_9Mo_{36}N_8O_{178}$	$C_{32}H_{190}As_4Co_9Mo_{36}N_8O_{178}$
Formula mass	7783.77	7819.72
Space group	$P\bar{1}$	$P\bar{1}$
a [Å]	14.2108(10)	14.102(2)
b [Å]	18.8804(13)	18.880(3)
c [Å]	22.5052(16)	22.783(3)
α [°]	71.6940(10)	71.074(3)
β [°]	83.8250(10)	83.106(3)
γ [°]	71.5560(16)	70.615(2)
V [$Å^3$]	5438.0(7)	5412.3(14)
Z	1	1
T [K]	183(2)	183(2)
Wavelength [Å]	0.71073	0.71073
$D_{calcd.}$ [M g m^{-3}]	2.338	2.331
T_{min}, T_{max}	0.328, 0.382	0.532, 0.805
Final R_1[a], wR_2[b] [$I > 2\sigma(I)$]	0.0646, 0.1203	0.0664, 0.1311
Final R_1[a], wR_2[b] [all data]	0.0815, 0.1272	0.1334, 0.1594

[a] $R_1 = \Sigma||F_o| - |F_c||/\Sigma|F_o|$. [b] $wR_2 = \{\Sigma[w(F_o^2 - F_c^2)^2]/\Sigma[w(F_o^2)^2]\}^{0.5}$.

CCDC-269468 (for **1**) and -269311 (for **2**) contain the supplementary crystallographic data for this paper. These data can be obtained free of charge from The Cambridge Crystallographic Data Centre via www.ccdc.cam.ac.uk/data_request/cif.

Electrochemical Experiments: The compositions of the various media used for UV/Vis spectroscopy were as follows: for pH 0, H_2SO_4; for pH 1–3, 0.2 M Na_2SO_4 + H_2SO_4; for pH 4 and 5, 0.4 M CH_3COONa + CH_3COOH. The test was realized on 2×10^{-6} M solutions of compound **1**. The solutions were deaerated thoroughly for at least 30 min with pure argon and kept under a positive pressure of this gas during the experiments.

Preparation of Compound 1-Modified Carbon Paste Electrode (CPE): Compound **1**-modified CPE was fabricated as follows: 0.5 g graphite powder and 0.05 g compound **1** were mixed, and ground together by an agate mortar and pestle to achieve an even, dry mixture; 0.50 mL paraffin oil was added to the mixture and stirred with a glass rod; then the mixture was packed into a glass tube with the diameter of 3 mm, and the surface was pressed tightly onto weighing paper with a copper rod through the back. Electrical contact was established with a copper rod through the back of the electrode.

Stability Studies: For identifying the solution stability of complex **1**, the UV/Vis spectrum of the solution was monitored as a function of pH over a period of at least 12 h at room temperature. The spectra reproducible with respect to shape, absorbance, and wavelength location over this period of time were considered to indicate complete stability.

Supporting Information (see also the footnote on the first page of this article): Several ball-and-stick representations, IR spectra, magnetic data and selected bond lengths angles for **1** and **2**.

Acknowledgments

The authors are thankful for the financial support from the National Natural Science Foundation of China (Grant numbers 20371010; 20671017) and the Specialized Research Fund for the Doctoral Program of Higher Education.

[1] a) M. T. Pope, A. Müller, *Angew. Chem. Int. Ed. Engl.* **1991**, *30*, 34–48; b) M. T. Pope, A. Müller (Eds.), *Polyoxometalates: from Platonic Solids to Anti Retroviral Activity*, Kluwer, Dordrecht, **1994**.
[2] a) C. L. Hill, C. M. Prosser-McCartha, *Coord. Chem. Rev.* **1995**, *143*, 407–455; b) C. L. Hill (Ed.), *Chemical Reviews, Polyoxometalates*, American Chemical Society, Washington, DC, **1998**.
[3] M. T. Pope, A. Müller (Eds.), *Polyoxometalate Chemistry: From Topology via Self-Assembly to Applications*, Kluwer, Dordrecht, The Netherlands, **2001**.
[4] T. Yamase, M. T. Pope (Eds.), *Polyoxometalate Chemistry for Nano-Composite Design*, Kluwer, Dordrecht, The Netherlands, **2002**.
[5] M. T. Pope, *Compr. Coord. Chem.* **2003**, *4*, 635–677.
[6] T. Liu, E. Diemann, H. Li, A. Dress, A. Müller, *Nature* **2003**, *426*, 59–62.
[7] T. Liu, *J. Am. Chem. Soc.* **2003**, *125*, 312–313.
[8] K. C. Kim, M. T. Pope, *J. Am. Chem. Soc.* **1999**, *121*, 8512–8517.
[9] X. Zhang, Q. Chen, D. C. Duncan, R. J. Lachicotte, C. L. Hill, *Inorg. Chem.* **1997**, *36*, 4381–4386.
[10] X. Zhang, T. M. Anderson, Q. Chen, C. L. Hill, *Inorg. Chem.* **2001**, *40*, 418–424.
[11] L. H. Bi, U. Kortz, B. Keita, L. Nadjo, H. Borrmann, *Inorg. Chem.* **2004**, *43*, 8367–8372.
[12] P. Mialane, J. Marrot, A. Mallard, G. Herve, *Inorg. Chim. Acta* **2002**, *238*, 81–86.
[13] a) I. M. Mbomekalle, B. Keita, L. Nadjo, K. I. Hardcastle, C. L. Hill, T. M. Anderson, *Dalton Trans.* **2004**, 4094–4095; b) L. H. Bi, M. Reicke, U. Kortz, B. Keita, L. Nadjo, R. J. Clark, *Inorg. Chem.* **2004**, *43*, 3915–3920; c) X. K. Fang, T. M. Anderson, W. A. Neiwert, C. L. Hill, *Inorg. Chem.* **2003**, *42*, 8600–8602; d) M. D. Ritorto, T. M. Anderson, W. A. Neiwert, C. L. Hill, *Inorg. Chem.* **2004**, *43*, 44–49.
[14] a) E. M. Limanski, D. Drewes, E. Droste, R. Böhner, B. Krebs, *J. Mol. Struct.* **2003**, *656*, 17–25; b) A. J. Gaunt, I. May, R. Copping, A. I. Bhatt, D. Collison, O. D. Fox, K. T. Holman, M. T. Pope, *Dalton Trans.* **2003**, 3009–3014; c) I. M. Mbomekalle, B. Keita, L. Nadjo, P. Berthet, W. A. Neiwert, C. L. Hill, M. D. Ritorto, T. M. Anderson, *Dalton Trans.* **2003**, 2646–2650.
[15] a) E. M. Limanski, M. Piepenbrink, E. Droste, K. Burgemeister, B. Krebs, *J. Cluster Sci.* **2002**, *13*, 369–379; b) L. Ruhlmann, J. Canny, R. Contant, R. Thouvenot, *Inorg. Chem.* **2002**, *41*, 3811–3819; c) T. M. Anderson, X. Zhang, K. I. Hardcastle, C. L. Hill, *Inorg. Chem.* **2002**, *41*, 2477–2488; d) A. C. Stowe, S. Nellutla, N. S. Dalal, U. Kortz, *Eur. J. Inorg. Chem.* **2004**, 3792–3797.
[16] H. F. Fukushima, A. Kobayashi, Y. Sasaki, *Acta Crystallogr., Sect. B: Struct. Sci.* **1981**, *37*, 1613–1615.
[17] A. Müller, E. Krickemeyer, S. Dillinger, J. Meyer, H. Bögge, A. Stammler, *Angew. Chem. Int. Ed. Engl.* **1996**, *35*, 171–173.
[18] A. Müller, E. Krickemeyer, M. Penk, V. Wittneben, J. Döring, *Angew. Chem. Int. Ed. Engl.* **1990**, *29*, 88–90.
[19] I. D. Brown, D. Altermatt, *Acta Crystallogr., Sect. B: Struct. Sci.* **1985**, *41*, 244–246.
[20] M. T. Pope, *Heteropoly and Isopoly Oxometalates*, Springer-Verlag, Berlin, **1983**, p. 101.
[21] R. A. Prados, M. T. Pope, *Inorg. Chem.* **1976**, *15*, 2547–2553.
[22] C. Sanchez, J. Livage, J. P. Launay, M. Fournier, *J. Am. Chem. Soc.* **1983**, *105*, 6817–6823.
[23] a) P. Mialane, A. Dolbecq, J. Marrot, E. Rivière, F. Sécheresse, *Eur. J. Inorg. Chem.* **2005**, 1771–1778; b) B. S. Bassil, S. Nellutla, U. Kortz, A. C. Stowe, J. van Tol, N. S. Dalal, B. Keita, L. Nadjo, *Inorg. Chem.* **2005**, *44*, 2659–2665.
[24] O. Kahn, *Molecular Magnetism*, VCH Verlagsgesellschaft, Weinheim, **1993**, p. 114.
[25] S. Q. Bai, E. Q. Gao, Z. He, C. J. Fang, C. H. Yan, *New J. Chem.* **2005**, *29*, 935.
[26] C. Sanchez, J. Livage, J. P. Launay, M. Fournier, Y. Jeannin, *J. Am. Chem. Soc*. **1982**, *104*, 3194–3202.

Received: June 3, 2006
Revised Version Received: February 21, 2007
Published Online: May 9, 2007

